J. Phys. A: Math. Gen., **13** (1980) 251–262. Printed in Great Britain

Renormalisation group study of a two-dimensional lattice model with directional bonding

B W Southern† and D A Lavis‡

Institut Laue–Langevin, 156X Centre de Tri, 38042 Grenoble Cedex, France
† Present address: Physics Department, University of Manitoba, Winnipeg, Manitoba, Canada R3T 2N2.
‡ On leave from Mathematics Department, Chelsea College, University of London, Manresa Road, London SW3 6LX, UK.

Received 5 March 1979

Abstract. Using real-space renormalisation-group methods we study the two-dimensional bonded lattice fluid model on a triangular lattice introduced by Bell and Lavis to describe the anomalous properties of water. We obtain the phase diagram for different values of the bonding strength. There are three different phases which correspond to the solid, liquid and gas phases of the model. The fixed points which control the transitions between these different phases are determined and the melting transition is found to be second-order in contrast to the predictions of mean-field theory. The molecular density and isothermal compressibility are calculated along an isobar which traverses all three phases and also along the coexistence curve and the results are compared with previous mean field calculations of these quantities.

1. Introduction

Since the work of Bernal and Fowler (1933) it has been widely recognised that many of the 'anomalous' properties of water arise from the competition between open and close-packed forms of molecular order which originates in the ability of the water molecule to form tetrahedrally directed hydrogen bonds. Bell and Lavis (1970) have considered a simple bonded-fluid model on a triangular lattice in which hydrogen bonding was represented by attributing to each molecule preferential bonding directions. Each molecule has three bonding arms at angles of 120° to each other and two distinct orientations in which the arms are directed towards nearest-neighbour sites. Since the molecules can be present or absent, each site can be in one of three possible states which may be represented by the spin states $S = \pm 1, 0$ of a spin-1 Ising model. Mean field calculations (Lavis 1973, 1975) and an exact transfer matrix treatment (Lavis 1976) of this model were able to reproduce some of the main features of the anomalous behaviour of water. The transition from the closed-packed liquid phase to the open (honeycomb) solid phase was found to be first-order with the characteristic decrease in density of the water–ice system.

In this paper we investigate the model using a block-spin real-space renormalisation group (RSRG) method (for a review see Niemeijer and van Leeuwen 1976). In order to preserve the sublattice ordering which occurs in the solid phase, we use the nine-site cluster employed by Schick *et al* (1977) in their study of the spin-$\frac{1}{2}$ Ising model and by

0305-4470/80/010251+12$01.00

Schick and Griffiths (1977) for the 3-state Potts model on the triangular lattice. The number of necessary coupling constants is determined by the size of the basic cluster and the symmetry of the model. In our case, we must consider a 6-dimensional space of couplings. The model is a slight generalisation of the Blume–Emery–Griffiths (1971) model which has been extensively studied using RSRG methods (Berker and Wortis 1976, Adler *et al* 1978, Mahan and Girvin 1978). With a suitable choice of relationships between the coupling constants, the Blume–Emery–Griffiths model reduces to a 3-state Potts model with a 2-dimensional coupling-constant subspace. The analogous special case of the Bell–Lavis model has a 3-dimensional subspace and this case has been studied by Young and Lavis (1979) using the same methods as in the present paper. They found all the fixed points in the extended Potts subspace and suggested that melting in the Bell–Lavis model is a second-order transition belonging to the same universality class as the ferromagnetic 3-state Potts model. However, our present calculations indicate that the melting transition does not belong to this universality class, although it is indeed second-order. The fact that the transition is continuous is unfortunate for the correspondence of the model with water, but this failure is probably associated more with the 2-dimensionality of the lattice than with its bonding structure.

We describe the model and the renormalisation group transformation in § 2. In § 3, the results for the phase diagram of the Bell–Lavis model are presented together with the fixed points and critical exponents describing the transitions between the gas, liquid and solid phases. The calculation of the thermodynamic functions is outlined in § 4 and a comparison is made of our present results with the previous mean-field and transfer-matrix calculations. Our conclusions are summarised in § 5.

2. The model

As indicated in the introduction, the three possible states of a site on the triangular lattice are represented by the states $S = \pm 1, 0$ of a spin-1 Ising model. The molecular states are identified with $S = \pm 1$, as shown in figure 1, and $S = 0$ represents a vacant state. A bonded pair of molecules has interaction energy $-(\epsilon + w)$ and an unbounded nearest- neighbour pair has interaction energy $-\epsilon$. In order to take proper account of sublattice orderings the lattice is divided into three equivalent sublattices A, B, C as indicated in figure 1. Within the grand canonical distribution with chemical potential μ, the Hamiltonian of the system is given by (Young and Lavis 1979)

$$\mathscr{H} = \sum_{\Delta} [-\tfrac{1}{6}\mu(S_A^2 + S_B^2 + S_C^2) + \tfrac{1}{8}w(S_A S_B + S_B S_C + S_C S_A) - \tfrac{1}{2}(\epsilon + \tfrac{1}{4}w)(S_A^2 S_B^2 + S_B^2 S_C^2 + S_C^2 S_A^2) + \tfrac{1}{8}w(S_A - S_B)(S_B - S_C)(S_C - S_A)] \quad (1)$$

where the summation is over all elementary triangles Δ of the lattice and $S_\alpha (\alpha = A, B, C)$ denotes the spin of the site on sublattice α in triangle Δ.

Apart from the final term in (1) this Hamiltonian has the same form as the Blume–Emery–Griffiths model. The special feature of the present model is exhibited by the final term which removes the degeneracy associated with cyclic and anti-cyclic ordering of the states $S = +1, 0, -1$ around an elementary triangle. For $w > 0$, cyclic ordering is favoured and this is the case that will be studied in this paper.

In any RSRG calculation all terms which will be generated by the recurrence relations must be included even if they are not present in the initial Hamiltonian. In our case,

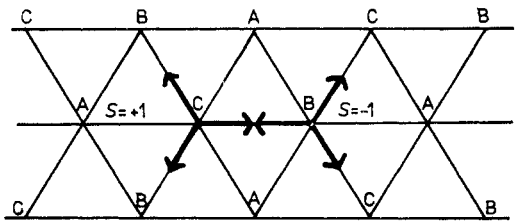

Figure 1. A portion of the triangular lattice showing the convention adopted for labelling the three sublattices A, B and C. A bonded pair of molecules is also shown with their corresponding spin states indicated.

these are simply all the terms which are invariant under simultaneous inversion ($S \to -S$) of all spins plus the final term in (1). Although this term is not invariant with respect to simultaneous inversion of all spins, it does not generate any new terms. In the general case, we have the Hamiltonian (Young and Lavis 1979)

$$-\beta\mathscr{H} = \sum_{\Delta} H_{\Delta} \qquad (\beta = 1/k_{\mathrm{B}}\mathrm{T}) \tag{2a}$$

with

$$\begin{aligned} H_{\Delta} = &-\tfrac{1}{6}\bar{\Delta}(S_{\mathrm{A}}^2 + S_{\mathrm{B}}^2 + S_{\mathrm{C}}^2) + \tfrac{1}{2}\bar{J}(S_{\mathrm{A}}S_{\mathrm{B}} + S_{\mathrm{B}}S_{\mathrm{C}} + S_{\mathrm{C}}S_{\mathrm{A}}) \\ &+ \tfrac{1}{2}\bar{K}(S_{\mathrm{A}}^2S_{\mathrm{B}}^2 + S_{\mathrm{B}}^2S_{\mathrm{C}}^2 + S_{\mathrm{C}}^2S_{\mathrm{A}}^2) + \bar{L}S_{\mathrm{A}}^2S_{\mathrm{B}}^2S_{\mathrm{C}}^2 \\ &+ \bar{M}S_{\mathrm{A}}S_{\mathrm{B}}S_{\mathrm{C}}(S_{\mathrm{A}} + S_{\mathrm{B}} + S_{\mathrm{C}}) - \tfrac{1}{4}\bar{\Omega}(S_{\mathrm{A}} - S_{\mathrm{B}})(S_{\mathrm{B}} - S_{\mathrm{C}})(S_{\mathrm{C}} - S_{\mathrm{A}}). \end{aligned} \tag{2b}$$

Comparing equations (1) and (2) we observe that the RSRG method generates two additional terms involving all three spins of the elementary traingles with coupling constants $\bar{L}$ and $\bar{M}$. The spectrum of H_{Δ} for each elementary triangle of the lattice has seven different configurations C_j with corresponding energies ϵ_j ($j = 1, 2, \ldots, 7$). These states are indicated in table 1 where the energies ϵ_j are given both in terms of the coupling constants of equation (2*b*) and also the original parameters of the model defined by (1).

We use the block spin transformation employed by Schick *et al* (1977) in their study of the spin-$\frac{1}{2}$ Ising model. An initial cluster of nine sites is chosen such that three sites belong to each of the three sublattices and periodic boundary conditions are applied. Application of the renormalisation group transformation reduces the nine-site cluster to a cluster of three sites, each one belonging to one of the three sublattices, and

Table 1. Spectrum of H_{Δ}.

Configuration C_j	Degeneracy ω_j	Energy ϵ_j	ϵ_j^0
C_1 $[0, 0, 0]$	1	0	0
C_2 $[\pm1, \pm1, \pm1]$	2	$-\bar{\Delta}/2 + 3\bar{J}/2 + 3\bar{K}/2 + \bar{L} + 3\bar{M}$	$\beta(\mu + 3\epsilon)/2$
C_3 $[0, 0, \pm1]$	6	$-\bar{\Delta}/6$	$\beta\mu/6$
C_4 $[0, \pm1, \pm1]$	6	$-\bar{\Delta}/3 + \bar{J}/2 + \bar{K}/2$	$\beta(2\mu + 3\epsilon)/6$
C_5 $[\pm1, \mp1, \mp1]$	6	$-\bar{\Delta}/2 - \bar{J}/2 + 3\bar{K}/2 + \bar{L} - \bar{M}$	$\beta(\mu + 3\epsilon + w)/2$
C_6 $[+1, 0, -1]_{\text{cyclic}}$	3	$-\bar{\Delta}/3 - \bar{J}/2 + \bar{K}/2 + \bar{\Omega}/2$	$\beta(2\mu + 3\epsilon + 3w)/6$
C_7 $[+1, -1, 0]_{\text{anticyclic}}$	3	$-\bar{\Delta}/3 - \bar{J}/2 + \bar{K}/2 - \bar{\Omega}/2$	$\beta(2\mu + 3\epsilon)/6$

corresponds to an increase in length scale by a factor of $\sqrt{3}$. To preserve the 3-state Potts symmetry of the model we adopt the weight function used by Schick and Griffiths (1977) and Young and Lavis (1979).

In addition to the Potts subspace, the Hamiltonian in (2) reduces to a spin-$\frac{1}{2}$ Ising model in two distinct limits. In the case $\mu \to \infty$ ($\bar{\Delta} \to -\infty$) the state $S = 0$ is suppressed and we have a nearest neighbour spin-$\frac{1}{2}$ Ising model with coupling constant $-\bar{J} - 2\bar{M} = -\beta w/4$. Our choice of weight function becomes equivalent to the 'majority rule' weight function of Schick *et al* (1977) in this limit and we obtain their results for the behaviour in the absence of a magnetic field and three spin couplings. That is, there is a ferromagnetic transition for $w < 0$ but no transition in the case $w > 0$ in agreement with the known exact results for the triangular lattice. Since we are concerned with this latter situation which favours bonding, the antiferromagnetic Ising model on the triangular lattice will correspond to the liquid phase of the model characterised by a large degree of short-range order, but no long-range order. This feature was also correctly obtained in the mean field approach of Lavis (1973). The second special case corresponds to the limit $\bar{J} = \bar{M} = \bar{\Omega} = 0$ where the distinction between $S = \pm 1$ is suppressed. If we define a new variable $t = 2S^2 - 1$ at each site (Griffiths 1967), then we may rewrite (2) as a spin-$\frac{1}{2}$ Ising model with both a magnetic field and three spin couplings present. In this limit our weight function for the S variables does not reduce to a 'majority rule' for the t variables since the symmetry between $t = \pm 1$ is not preserved.

Defining the variables

$$x_j = \exp(\epsilon_j) \qquad (j = 1, 2, \ldots, 7) \tag{3}$$

the recurrence relations can be written in the form

$$(x_j')^6 = G(x_1, x_2, \ldots, x_7) \sum_{\{n_i\}} P_j(\{n_i\}) x_1^{n_1} x_2^{n_2} \ldots x_7^{n_7} \tag{4}$$

where n_i is the number of triangles in the nine-site cluster in state C_i of table 1, $P_j(\{n_i\})$ is the degeneracy associated with $\{n_i\}$ and $G(x_1, x_2, \ldots, x_7)$ is given by the condition $x_1 = x_1' = 1$. The parameter G is a constant term in the Hamiltonian generated at each iteration of (4) and will be used in § 4 to calculate the thermodynamic functions. We start with values of the x_j variables in (3) related to the coupling constants of the model in (1) as in table 1. The recurrence relations (4) then determine trajectories in the full 6-dimensional space of couplings. A trajectory which starts at a point where the behaviour of the system is not critical will iterate to a sink which characterises that phase. These regions are separated by the critical regions which form domains of attraction for the critical fixed points. Once these fixed points have been located the recurrence relations can be linearised about the fixed points and the eigenvalues λ_i of the linear equations can be calculated. The critical exponents y_i are related to the eigenvalues by $\lambda_i = b^{y_i}$ where b is the scale factor and is equal to $\sqrt{3}$ in the present calculation.

3. Phase diagram and critical behaviour

The behaviour at zero temperature of the model defined in equation (1) can be obtained most easily by comparing the ground-state energies of the seven possible configurations of each elementary triangle. These energies are given in terms of the parameters μ, w and ϵ in the final column of table 1. In our analysis we shall only consider the cases for

which both $\epsilon \geqslant 0$ and $w \geqslant 0$ since this corresponds to the situation in water where hydrogen bonding is believed to play an important role.

In the absence of bonding, i.e. $w = 0$, the stable configuration at zero temperature is the vacant state C_1 if $\mu < -3\epsilon$ whereas the close-packed states C_2 and C_5 are most stable if $\mu > -3\epsilon$. As the strength of the bonding parameter w increases from zero, the ground state characteristics of the system remain qualitatively unchanged until $w = 3\epsilon$. The only difference for $0 < w < 3\epsilon$ is that the degeneracy between the states C_2 and C_5 is lifted and C_5 is the most stable configuration if $\mu > -3\epsilon + w$. However, for values of w larger than 3ϵ, there is a range of the parameter μ in which the open (honeycomb) bonded phase is the stable ground state and this is represented by the state C_6 of table 1. The condition for C_6 to be the most stable phase is determined by $-\frac{3}{2}(\epsilon + w) < \mu < -6\epsilon$. The vacant state C_1 is most stable for $\mu < -\frac{3}{2}(\epsilon + w)$ and the close-packed state C_5 is most stable for $\mu > -6\epsilon$. Since the molecular number densities of the states C_1, C_6 and C_5 are 0, $\frac{2}{3}$ and 1 respectively, they correspond to the gas, solid and liquid phases of the Bell–Lavis model. The liquid ground state C_5 is highly degenerate having the same ground state entropy as the spin-$\frac{1}{2}$ Ising antiferromagnet on a triangular lattice (Bell and Lavis 1970).

The domains of these three phases at finite temperature correspond to the domains of attraction of the corresponding sinks of the recurrence relations in equation (4). In terms of the variables x_j defined in equation (3), the sinks for the solid and gas phases are $x_j/x_6 \to \delta_{j6}$ and $x_j/x_1 \to \delta_{j1}$ respectively. The sink for the liquid phase at zero temperature is a special fixed point, $x_j/x_5 = \delta_{j5}$, and is accessible only for trajectories which begin at zero temperature. It is the same fixed point as AF′ that was found in the work of Schick *et al* (1977). However, at any finite temperature in the liquid phase all trajectories iterate to a sink given by $x_j/x_5 \to (\delta_{j2} + \delta_{j5})$. A numerical study of the trajectory flows allows us to construct the phase diagram and to determine the boundaries which separate one phase from another.

Our results for the phase diagram in the case $w = 0$, where the bonded solid phase is not energetically favoured, are shown in figure 2(*a*) as a function of the reduced

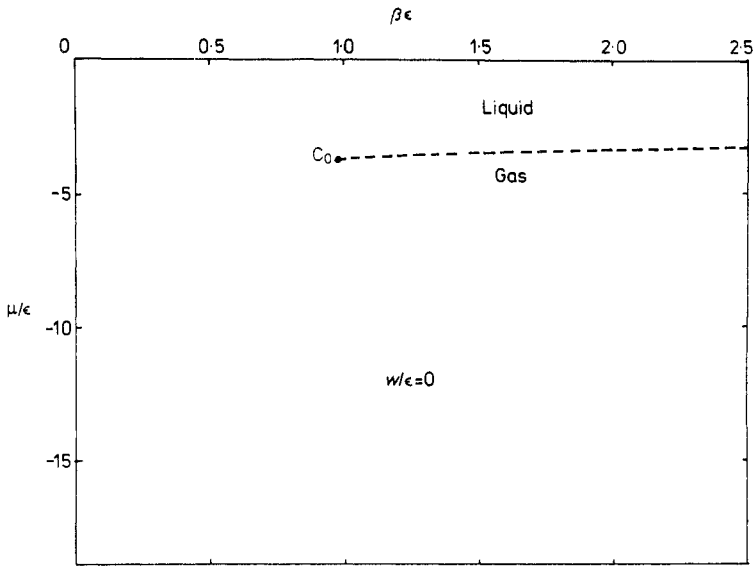

Figure 2(*a*).

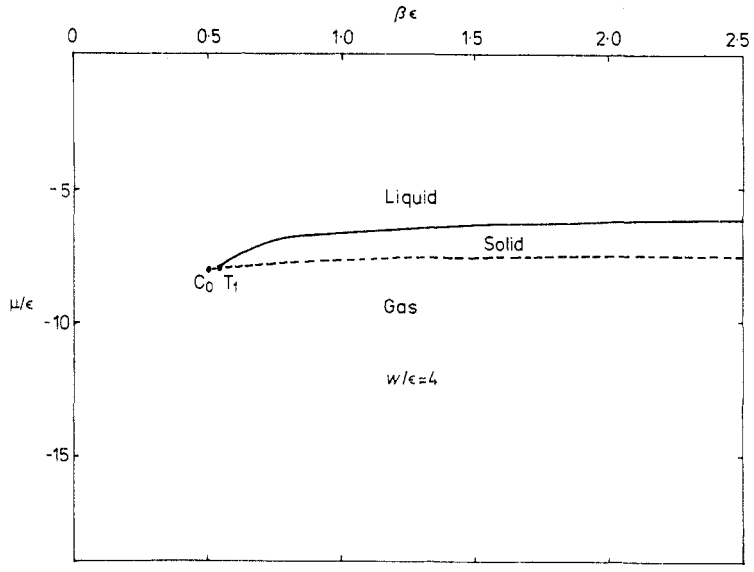

Figure 2(*b*).

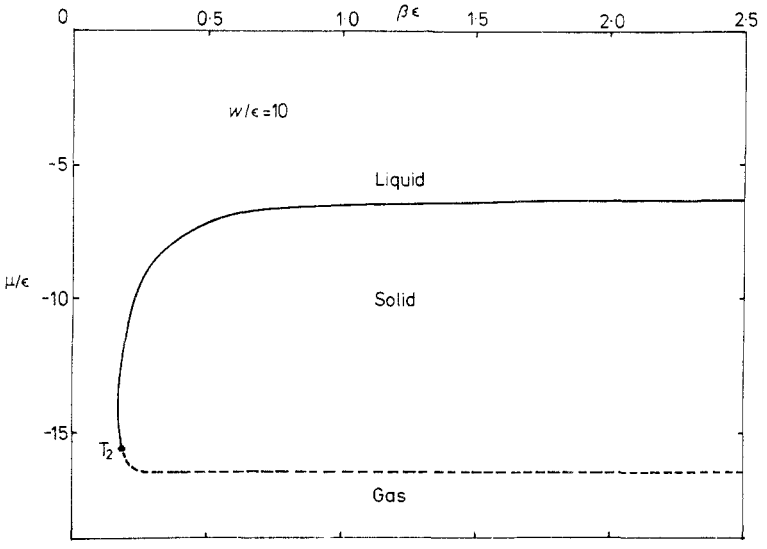

Figure 2(*c*).

Figure 2. Phase diagram for the Bell–Lavis model in terms of the variables μ/ϵ and $\beta\epsilon$ for different values of the ratio w/ϵ: (*a*) $w/\epsilon = 0$, (*b*) $w/\epsilon = 4$ and (*c*) $w/\epsilon = 10$. First-order boundaries are indicated by dashed lines and second order boundaries by full lines. The critical end-point for the liquid–gas transition is designated by C_0 in (*a*) and (*b*) while the point where all three phases meet is designated by T_1 and T_2 in (*b*) and (*c*) respectively.

variables μ/ϵ and $\beta\epsilon$. We find a first-order phase boundary (broken curve) separating the gas and liquid phases. This boundary asymptotically approaches $\mu/\epsilon = -3$ as $\beta\epsilon \to \infty$ and terminates at a critical end point C_0 at a finite temperature. The first-order transition is controlled by a discontinuity fixed point LG which has a characteristic

relevant exponent $y_1 = d = 2$ (Nienhuis and Nauenberg 1975). The critical end point C_0 lies in the domain of attraction of a second fixed point X which has two relevant exponents. The coordinates and exponents of these fixed points are given in table 2.

Figure 2(*b*) shows the phase diagram for the case $w = 4\epsilon$. The solid phase now appears between the liquid and gas phases at low temperatures. We have chosen this value of w in order to compare our results with the mean-field calculations of Lavis (1973). However, we shall postpone a detailed comparison until § 4. The liquid–solid transition in figure 2(*b*) is second-order and controlled by the fixed point LS of table 2 which has only one relevant exponent. The gas–solid transition is first-order and controlled by the discontinuity fixed point GS while the liquid–gas transition at temperatures below the critical end-point C_0 is again controlled by LG with the transition at C_0 described by fixed point X. These three phase boundaries meet in figure 2(*b*) at the point T_1 which lies within the domain of attraction of fixed point Y of table 2. This latter fixed point has two relevant exponents and describes the meeting of one critical and two first-order surfaces. The exponents exhibit typical critical end-line behaviour (Berker and Wortis 1976), combining a leading $y_1 = d = 2$ with a $y_2 = 1{\cdot}129$ in close agreement with the leading exponent of LS.

Figure 2(*c*) shows our results in the case $w = 10\epsilon$. At this larger value of the bonding strength the phase diagram is qualitatively different from that shown in figure 2(*b*). The first-order transition between the liquid and gas phases has disappeared but the gas–solid and liquid–solid transitions are still described by the fixed points GS and LS respectively. These two phase boundaries meet at point T_2 in figure 2(*c*) and this point lies in the domain of attraction of fixed point AF^+. This latter fixed point is situated in the extended Potts subspace studied previously in the paper by Young and Lavis (1979) and it has two relevant exponents. The changeover from the type of behaviour shown in figure 2(*b*) to that found in figure 2(*c*) occurs at an intermediate value of w when the domains of attraction of fixed points X, Y and AF^+ intersect at a point T_3. This point lies in the domain of attraction of the fixed point Z of table 2 which possesses three relevant exponents and describes the intersection of two first-order and two second-order surfaces.

Melting in the Bell–Lavis model is thus found to be a second-order phase transition in contrast to the mean-field calculations which predicted a first-order transition. However, this difference may be a consequence of the low dimensionality of the lattice. Mean-field theory also predicts a first-order transition for the ferromagnetic 3-state Potts model in two dimensions, whereas exact results obtained by Baxter (1973) show that it has a continuous transition. Our results are not in accord with the suggestion by Young and Lavis (1979) that the melting transition in the Bell–Lavis model belongs to the same universality class as the ferromagnetic 3-state Potts model. However, for large enough values of the bonding strength w, the point on the phase boundary where the second-order liquid–solid curve meets the first order gas–solid curve does indeed belong to this universality class.

4. Thermodynamic functions

The partition function Z associated with the initial cluster of nine sites is given by

$$Z = \sum_j \omega_j \sum_{\{n_i\}} P_j(\{n_i\}) x_1^{n_1} x_2^{n_2} \ldots x_7^{n_7} \tag{5}$$

Table 2. Fixed points and exponents.

Designation	Location							Exponents					
	x_1	x_2	x_3	x_4	x_5	x_6	x_7	y_1	y_2	y_3	y_4	y_5	y_6
X	1	0·689	0·496	0·515	0·689	0·515	0·515	1·761	0·697	−0·708	−1·151	−1·285	−2·388
Y	1	0·453	0·076	0·213	0·736	0·919	0·171	2	1·129	−0·388	−0·388	−1·827	−1·960
Z	1	0·478	0·376	0·406	0·684	0·938	0·369	1·945	1·097	0·534	−0·683	−1·404	−1·902
AF^+	1	1	1·172	1·172	1·172	2·051	1	1·036	0·327	−0·983	−1·583	−1·793	−2·124
LS	1	20·721	3·373	9·743	33·680	42·017	7·790	1·129	−0·391	−0·391	−1·881	−2·013	−3·687
LG	1	0·707	0	0	0·707	0	0	2	−0·524	−1·052	−1·052	−1·052	$-\infty$
GS	1	0	0	0	0	1	0	2	$-\infty$	$-\infty$	$-\infty$	$-\infty$	$-\infty$

where the ω_j are degeneracy factors associated with the configurations of each elementary traingle and are listed in table 1. The remaining quantities are the same as those appearing in equation (4). After the renormalisation group transformation (4) has been applied, the partition function Z' associated with the remaining cluster of three sites is simply

$$Z = \sum_j \omega_j (x_j')^6. \tag{6}$$

Using (4) we find that the free energies per site are related as follows,

$$f = \tfrac{1}{9} \ln G + \tfrac{1}{3} f' \tag{7}$$

where $f = -\frac{1}{9} \ln Z$, $f' = -\frac{1}{3} \ln Z'$ and G is a constant term generated at each iteration of the recurrence relations in (4). Iterating (7), we find that the free energy per site (in units of $k_B T$) can be written in the form

$$f^{(0)} = \tfrac{1}{9} \sum_{l=0}^{\infty} \frac{1}{3^l} \ln G^{(l)} \tag{8}$$

In practice, the infinite series converges very quickly and the free energy at any initial values of the x_j defined in (3) can be obtained after only a few iterations. Similarly, the derivatives of the free energy $f^{(0)}$ can be obtained using a chain-rule of differentiation (see Niemeijer and van Leeuwen 1976 for details).

In the case of the model under study, the pressure P of the system is obtained from $f^{(0)}$ in (8) as follows

$$PV_0 = -k_B T f^{(0)} \tag{9}$$

where V_0 is the two-dimensional volume per lattice site. The pressure at any point in the phase diagrams of figure 2 can be calculated and, in particular, the value of the pressure on the boundaries which separate the phases. In this section we shall consider only the case $w = 4\epsilon$. Figure 3 shows our results for the phase diagram of figure 2(b) plotted as a function of PV_0/ϵ and $k_B T/\epsilon$. The mean field results (Lavis 1973) as well as the exact matrix calculations (Lavis 1976) are also plotted for comparison. Although no phase transitions occur in the matrix calculations, the maxima in the compressibility can be regarded as incipient phase transitions. The principal difference between our results and the mean field calculations is that we find a second-order transition between the solid and liquid phases.

The molecular number density ρ is given by

$$\rho = \left(\frac{\partial P}{\partial \mu}\right)_T V_0 = \frac{\partial f^{(0)}}{\partial \bar{\Delta}} \tag{10}$$

and the isothermal compressibility K_T is obtained from

$$K_T = \frac{V_0}{\rho^2}\left(\frac{\partial \rho}{\partial \mu}\right)_T = -\frac{\beta V_0}{\rho^2} \frac{\partial^2 f^{(0)}}{\partial \bar{\Delta}^2}. \tag{11}$$

Figure 4 shows the density and compressibility along the isobar $PV_0/\epsilon = 0{\cdot}1$. This is an isobar which passes through all three phases of the system as the temperature is varied. At the highest temperatures the system is in the gas phase and a first-order transition from gas to liquid occurs on lowering the temperature with corresponding discontinuities in ρ and K_T. At lower temperatures there is a second transition from the

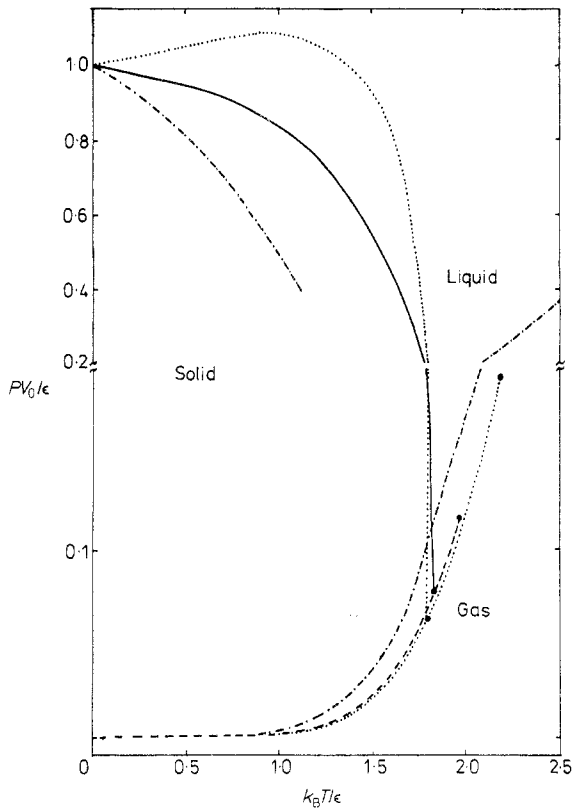

Figure 3. Pressure–temperature phase diagram of the Bell–Lavis model corresponding to the case $w/\epsilon = 4$ of figure 2(b). Our results are indicated by the full and broken curves. The results of the mean field treatment are indicated by the dotted lines and the exact matrix calculation results by the chain lines. The scale of the vertical axis changes by a factor of 5 at $PV_0/\epsilon = 0{\cdot}2$.

liquid to the solid phase with no discontinuity in density. The compressibility K_T diverges weakly with an exponent γ which is related to the relevant exponent of the fixed point LS of table 2 as follows: $\gamma = 2(y_1 - 1)/y_1$ and has the value 0·2289. Notice that there is a density maximum on the isobar but that it occurs in the solid rather than in the liquid phase as would be the case for the water system (Eisenberg and Kauzmann 1969 p 183). This particular weakness of the model was also present in the mean-field calculations of Lavis (1973) where the density maximum occurred in the metastable liquid phase at a temperature below the freezing temperature. We have, however, obtained a compressibility minimum in the liquid phase although this is probably a direct result of the singular behaviour at the solid–liquid transition. In water this minimum occurs with a discontinuity in K_T at the water–ice transition (Eisenberg and Kauzmann 1969 p 184).

Figure 5 shows our results for the isothermal compressibility along the liquid–solid side of the first order boundary T_1C_0 of figure 2(b). The exponent γ which describes the divergence of K_T as the critical end point C_0 is approached along the coexistence curve is given in terms of the relevant exponents of fixed point X and has the value $\gamma = 2(y_1 - 1)/y_2 = 2{\cdot}1847$. However, as T_1 is approached along the coexistence curve,

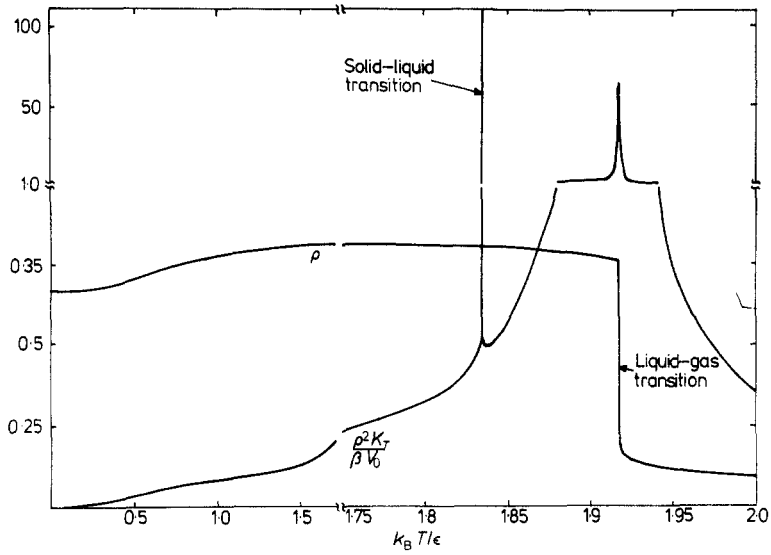

Figure 4. The quantities ρ and $\rho^2 K_T/\beta V_0$ along the isobar $PV_0/\epsilon = 0{\cdot}1$ are shown as a function of $k_B T/\epsilon$. The vertical scale changes by a factor of 200 at the value 1·0 and the horizontal scale changes by a factor of 10 at $k_B T/\epsilon = 1{\cdot}75$.

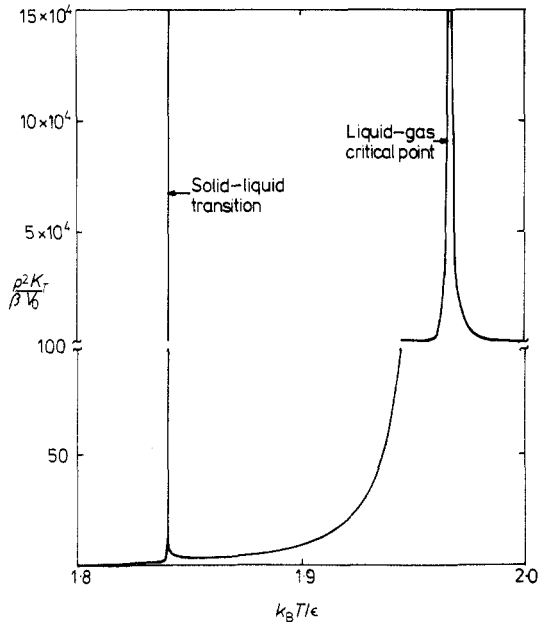

Figure 5. The quantity $\rho^2 K_T/\beta V_0$ along the solid and liquid sides respectively of the solid–gas and liquid–gas coexistence curve is shown as a function of $k_B T/\epsilon$. The vertical scale changes by a factor of 10^3 at the value 100.

the value of γ is determined by the exponents of fixed point Y and has the value $\gamma = 2(y_2 - 1)/y_2 = 0{\cdot}2288$. This latter value of γ is, as might be expected, very close to that for the liquid–solid transition along an isobar. Of course, the isothermal compressibility must have a minimum along the coexistence curve between the two singularities.

This is also the case for the water system (Rowlinson 1969 p 55) but it is difficult to regard this as a success for the Bell–Lavis model in view of the second-order nature of the liquid–solid transition.

5. Conclusions

We have studied the Bell–Lavis model of a bonded lattice fluid on a triangular lattice using RSRG techniques. In contrast to the mean-field calculations for this model, we find that the transition between the solid and liquid phase is second-order. However, this difference is most likely due to the low dimensionality of the lattice. Although the two-dimensional bonding model does not correctly describe the melting transition that is observed in water, a three-dimensional bonding model such as that proposed by Bell (1972) for a BCC lattice may in fact provide a more realistic description. We are presently investigating this latter model using RSRG techniques.

References

Adler J, Aharony A and Otimaa J 1978 *J. Phys. A: Math. Gen.* **11** 963–74
Baxter R J 1973 *J. Phys. C: Solid St. Phys.* **6** L445–8
Bell G M 1972 *J. Phys. C: Solid St. Phys.* **5** 889–905
Bell G M and Lavis D A 1970 *J. Phys. A: Gen. Phys.* **3** 568–81
Berker A N and Wortis M 1976 *Phys. Rev.* B **14** 4946–63
Bernal J D and Fowler R H 1933 *J. Chem. Phys.* **1** 515–48
Blume M, Emery V J and Griffiths R B 1971 *Phys. Rev.* A **4** 1071–7
Eisenberg D and Kauzmann W 1969 *The Structure and Properties of Water* (London: Oxford University Press)
Griffiths R B 1967 *Physica (Utrecht)* **33** 689–90
Lavis D A 1973 *J. Phys. C: Solid St. Phys.* **6** 1530–45
—— 1975 *J. Phys. A: Math. Gen* **8** 1933–51
—— 1976 *J. Phys. A: Math. Gen.* **9** 2077–95
Mahan G D and Girvin S M 1978 *Phys. Rev.* B **17** 4411–5
Niemeijer Th and van Leeuwen J M J 1976 *Phase Transitions and Critical Phenomena* vol. 6 ed C Domb and M S Green (NY: Academic) pp 425–505
Nienhuis B and Nauenberg M 1975 *Phys. Rev. Lett.* **35** 477–9
Rowlinson J S 1969 *Liquids and Liquid Mixtures* (London: Butterworths)
Schick M and Griffiths R B 1977 *J. Phys. A: Math. Gen.* **10** 2123–31
Schick M, Walker J S and Wortis M 1977 *Phys. Rev.* B **16** 2205–19
Young A P and Lavis D A 1979 *J. Phys. A: Math. Gen.* **12** 229–43